Neurochemical Research (2019) 44:1375–1386
https://doi.org/10.1007/s11064-018-2657-x

ORIGINAL PAPER

Platelets Bioenergetics Screening Reflects the Impact of Brain Aβ Plaque Accumulation in a Rat Model of Alzheimer

Federico A. Prestia[1] · Pablo Galeano[1] · Pamela V. Martino Adami[1] · Sonia Do Carmo[2] · Eduardo M. Castaño[1] · A. Claudio Cuello[2] · Laura Morelli[1]

Received: 30 May 2018 / Revised: 26 September 2018 / Accepted: 6 October 2018 / Published online: 24 October 2018

Abstract

Alzheimer's disease (AD) is associated to depressed brain energy supply and impaired cortical and hippocampal synaptic function. It was previously reported in McGill-R-Thy1-APP transgenic (Tg(+/+)) rats that Aβ deposition per se is sufficient to cause abnormalities in glucose metabolism and neuronal connectivity. These data support the utility of this animal model as a platform for the search of novel AD biomarkers based on bioenergetic status. Recently, it has been proposed that energy dysfunction can be dynamically tested in platelets (PLTs) of nonhuman primates. PLTs are good candidates to find peripheral biomarkers for AD because they may reflect in periphery the bioenergetics deficits and the inflammatory and oxidative stress processes taking place in AD brain. In the present study, we carried out a PLTs bioenergetics screening in advanced-age (12–14 months old) control (WT) and Tg(+/+) rats. Results indicated that thrombin-activated PLTs of Tg(+/+) rats showed a significantly lower respiratory rate, as compared to that measured in WT animals, when challenged with the same dose of FCCP (an uncoupler of oxidative phosphorylation). In summary, our results provide original evidence that PLTs bioenergetic profiling may reflect brain bioenergetics dysfunction mediated by Aβ plaque accumulation. Further studies on human PLTs from control and AD patients are required to validate the usefulness of PLTs bioenergetics as a novel blood-based biomarker for AD.

Keywords Alzheimer's disease · Brain dysfunction · Platelet bioenergetic · Transgenic rat · Amyloid β · Blood-based bioenergetic profiling

Introduction

The global social and economic impact of Alzheimer's disease (AD) is staggering. It is estimated that in 2050, 115 million people will suffer from this type of dementia. While mortality rates from other major diseases, including acute myocardial infarction and stroke, have significantly decreased in recent years, deaths due to AD have increased by 68% between 2000 and 2010 [1]. More than two decades ago, the FDA authorized the administration of drugs with symptomatic benefits in AD. However, compounds based on the elimination of amyloid peptide β (Aβ), developed under the causal amyloid hypothesis which has dominated the research field over the last 30 years [2], have shown to be ineffective. In addition, there is a growing consensus suggesting that specific treatments for AD should be administered in subjects with genetic and metabolic risk factors before the onset of clinical symptoms [3]. Peripheral biomarkers are essential to make rapid and reliable diagnoses in

Special issue: In honor of Prof. Anthony J. Turner.

Electronic supplementary material The online version of this article (https://doi.org/10.1007/s11064-018-2657-x) contains supplementary material, which is available to authorized users.

✉ Laura Morelli
lmorelli@leloir.org.ar

[1] Laboratory of Amyloidosis and Neurodegeneration, Fundación Instituto Leloir, IIBBA-CONICET, Av. Patricias Argentinas 435, C1405BWE Ciudad Autónoma de Buenos Aires, Argentina

[2] Department of Pharmacology and Therapeutics, McGill University, McIntyre Medical Building 3655 Prom. Sir-William-Osler, Montreal, QC H3G 1Y6, Canada

different types of diseases. In AD, the identification of antemortem molecular characteristics is problematic. The available validated core biomarkers (Aβ42/Aβ40 ratio and p-Tau levels) are assessed in cerebrospinal fluid (CSF), a material not suitable for routine diagnosis. On the other hand, the best method to evaluate in vivo brain glucose metabolism impairments and Aβ deposition is the Positron Emission Tomography (PET) [4] with fluordeoxyglucose (FDG) or with any of the Aβ tracers currently available, respectively. However, PET is a very expensive procedure, making its widespread use unfeasible. As a result, there is a growing demand for peripheral biomarkers from more accessible samples. In this sense, it is thought that the development and validation of blood-based biomarkers would greatly facilitate the diagnosis of AD. Plasma is a sample that can be non-invasively and economically obtained, but until now biomarkers detected in plasma have not been validated for routine use in AD diagnosis [5]. In this context, platelets (PLTs) constitute an attractive alternative for the search of peripheral biomarkers for AD because they share biochemical properties with neurons [6, 7] and previous studies have shown that they recapitulate brain abnormalities present in psychiatric and neuronal disorders [8].

PLTs, one of the main elements of blood together with erythrocytes and leukocytes, are generated from nucleated precursor cells (megakaryocytes) in the bone marrow and delivered in the bloodstream without nuclei [9]. PLTs are metabolically active cells, containing numerous functional organelles, such as endoplasmic reticulum, Golgi apparatus, and mitochondria. They have a wide array of surface receptors and adhesion molecules, and contain numerous granules. Circulating unactivated (*resting*) PLTs are biconvex discoid structures (2–3 μm in its greatest diameter) with a half-life of 8–12 days. The term "*PLTs dynamics*" involves the complex process of converting *resting* PLTs into a PLTs plug, which most important function is to ensure hemostasis (prevention of blood loss when small blood vessels break accidentally). At the physiological level, PLTs activation is stimulated by bound PLTs secretion products and local prothrombotic factors, such as tissue factor. Multiple pathways can lead to PLTs activation in vivo [10] and most soluble agonists released by cells, such as ADP, thromboxane A2 (TxA2) and thrombin, trigger PLTs activation in vivo and in vitro. Thrombin is one of the strongest PLTs agonist and exerts its action through G protein-coupled protease-activated receptors (PARs), which are highly expressed on PTLs surface [11]. Moreover, recent studies suggest that in addition to their common function in the regulation of thrombosis and hemostasis, PLTs also contribute to tissue inflammation affecting adaptive immunity [12].

More than 30 years ago, it was reported that human PLTs express amyloid precursor protein (APP) and all the enzymatic machinery required to process APP through the same pathways described in brain to generate Aβ [13]. Since then, a large body of evidence has been accumulated suggesting that PLTs may be a good peripheral model to study APP metabolism and the pathophysiology of AD [14]. Two major theories have been proposed about the origin of Aβ in blood. One suggests that Aβ is derived from the central nervous system through the blood-CSF barrier and then absorbed onto the surface of PLTs [15], and the other theory proposes that there is an additional release of Aβ from blood cells, including PLTs, and from other non-neuronal cells [16]. However, the role of PLTs in AD still remains debated and controversial.

Interestingly, it was recently shown that the functionality of PLTs mitochondria positively correlates with brain glucose metabolism in African Green monkeys [17], supporting the notion that energetic brain functionality can be tested dynamically in PLTs [18]. Bioenergetics has become a crucial concept in neurodegenerative and cardiovascular diseases, diabetes, asthma, pulmonary hypertension and cancer. It is involved in pathological mechanisms, in development of new therapeutic strategies and as a potential biomarker for the progression of these disorders. A key concept is that mitochondria from PLTs can act as a "*sentinel*", serving as an early warning of the bioenergetic crisis in the brain of subjects susceptible to AD. Taking advantage of its precocity and sensitivity, bioenergetic monitoring has been proposed as a necessary factor to determine the severity and progression of complex and multifactorial disorders, including AD.

Although animal models have provided essential insights into the molecular mechanisms of AD [19], no reports have addressed PLTs biology in the most common AD transgenic rodent models. One possible explanation for this situation is that the promoters used in the construction of the transgen circumscribe the expression of the human mini gen to the brain, thus excluding megakariocytes from bone marrow and downplaying the role of rodent PLTs in these animal models.

In the present study, we address whether PLTs respiration may be used as a measurable proxy of bioenergetic alterations described in the homozygous variant of the McGill-R-Thy1-APP transgenic (Tg(+/+)) rat. We employed this animal model because it captures the full array of AD-like amyloid pathology, including intraneuronal Aβ accumulation, senile plaques, gliosis and memory impairments from the early adulthood onwards [20]. Moreover, by using PET and hippocampal volumetry, a longitudinal, multimodal imaging study was performed in this animal model for quantifying age-dependent brain Aβ deposition, progressive synaptic dysfunction and cognitive impairment. Results emphasize the impact of Aβ on brain functionality and support the notion that Aβ aggregation itself is sufficient to impose metabolic brain dysfunction [21]. Here we show that Aβ accumulation in Tg(+/+) brains is reflected by decrements

on the respiratory rate of thrombin-activated PLTs as compared to control animals. This preliminary report provides experimental evidence supporting PLTs bioenergetics profiling as a potential biomarker of brain metabolism alterations that have been linked to the development of AD.

Materials and Methods

Reagents

Diamidino-2-phenylindole (DAPI) and isofluorane were purchased from Life Technologies and Piramal, respectively. Sodium citrate, pyruvate, D-glucose, L-glutamine and thrombin isolated from human plasma were from Sigma-Aldrich. Oligomycin A, carbonyl cyanide *p*-(trifluoro-methoxy) phenyl-hydrazone (FCCP), and rotenone/antimycin A were provided by Seahorse Bioscience.

Animals and Ethical Statement

McGill-R-Thy1-APP homozygous transgenic (Tg(+/+)) rats harboring the human APP751 transgene with the Swedish and Indiana mutations under the control of the murine Thy1.2 promoter [20] were provided to Fundación Instituto Leloir (FIL) by The Royal Institution for the Advancement of Learning/McGill University Montreal, Quebec (Canada) after signing a Material Transfer Agreement to proceed with the experimental research. Tg(+/+) and age-matched wild-type (WT) littermates were maintained in polycarbonate cages in a temperature-controlled animal facility with a 12-h dark/light cycle and allowed to consume deionized water and a basal diet that provided all known required nutrients in sufficient quantities to provide maximal growth. Experiments were performed with male rats of two different range of age: 3–6 months old and 12–14 months old. The study was carried out in strict accordance with the ARRIVE (Animal Research: Reporting of In Vivo Experiments) and the OLAW-NIH (Office Laboratory Animal Welfare) guidelines. The protocol was approved by the local Animal Care Committee of Fundación Instituto Leloir (FIL) Assurance # A5168-01.

Platelets (PLTs) Isolation and Characterization

Tg(+/+) and WT rats (n = 4–6/group) were anesthetized by isofluorane inhalation and after being placed in a guillotine blade and beheaded, blood (10 mL) was collected in sterile tubes containing ACD buffer (39 mM citric acid, 75 mM sodium citrate, 135 mM dextrose, pH 7.4). PLTs were isolated by differential centrifugation as previously described [22]. Briefly, whole blood was centrifuged (250×*g* for 15 min) to obtain platelet-rich plasma (PRP). PLTs were isolated by sequential centrifugation of PRP (900×*g*/15 min) at room temperature to avoid PLTs activation. Then, PLTs were resuspended in modified Tyrode buffer (20 mM HEPES, 128 mM NaCl, 12 mM bicarbonate, 0.4 mM NaH2PO4, 5 mM glucose, 1 mM MgCl2, 2.8 mM KCl, pH 7.4) containing 0.5% bovine serum albumin. PLTs concentration and indices including analyser-calculated measure of thrombocyte volume (MPV); mean platelet mass (MPM), indicator of volume variability in platelets size (PDW), volume occupied by platelets in the blood (PCT), measure of mean refractive index of the platelets (MPC) were obtained using an auto hematology analyzer Advia 2120 (Siemens). Coagulogram was performed with a Destiny 100 (Tcoag) instrument. Standardization of rat blood clotting tests with reagents used for humans was performed according to a previous report [23].

Platelets (PLTs) Aggregation

The test was performed by a turbidimetric method as previously described [24] in a Lumiaggregometer (Chrono-Log, Havertown, PA, USA). Briefly, platelet-rich plasma (PRP) was obtained as described above and then the remaining blood sample was centrifuged for 15 min at 1000×*g* to recover platelet-poor plasma (PPP), which was used as control. All tests were performed within 2 h after PRP and PPP preparation. Platelet count in the PRP samples was adjusted with RPMI buffer to be between 250×10^3 and 300×10^3 PLTs/µL. The reaction was performed at constant temperature (37 °C). Three hundred and fifty µL of adjusted PRP were used for the analysis and the addition of the agonist (thrombin) was performed while stirring. PRP was stimulated with a final concentration of 1 Unit of human thrombin and PLTs aggregation was recorded for 140 s with PPP as blank control.

Biochemical Characterization of Platelets (PLTs)

To estimate mitochondria mass in PLTs preparations, PLTs pellets were homogenized in 0.5 mL of RIPA buffer (150 mM NaCl, 0.5% sodium deoxycholate, 1% TritonX-100, 2% SDS) containing proteases inhibitors (5 mM EDTA, 5 mM EGTA, 5 µg/mL leupeptin, 10 µg/mL aprotinin, 1 µg/mL pepstatin) and phosphatases inhibitors (50 mM sodium fluoride and 5 mM sodium orthovanadate) and centrifuged at 20,000×*g* at 4 °C for 45 min using an Eppendorf microcentrifuge. Supernatants were aliquoted and stored at − 80 °C until used. Protein concentration was determined using Pierce BCA Protein Assay Kit (Thermo Scientific) and samples (20–35 µg/lane) were run in SDS-Tricine 12.5% gels and transferred to PVDF membranes. Membranes were stained with Ponceau S to get an overview of total protein in each lane, blocked with 5% skim

milk in PBS for 1 h at room temperature and then incubated overnight at 4 °C with mouse anti-ATP synthase β-subunit (1:1000, Life Technologies) and mouse anti-β actin (1:20,000, Sigma). Peroxidase-conjugated secondary antibody and enhanced chemiluminescence detection system (ECL, Thermo Scientific) were used to detect immunoreactivity which was quantitated with a STORM 840 Phosphor Imager (GE Healthcare). Individual samples of PLTs were grouped by transgene status. PLTs corresponding to Tg(+/+) (n = 3) and WT (n = 3) were analyzed.

Metabolic Profiling in Resting and Thrombin Activated Platelets

PLTs (15×10^6/well) were loaded in unbuffered Dulbecco's Modified Eagle Medium (DMEM) into each well of an XFp microplate pre-coated with polyethylenimine (PEI) to measure the cell respiratory control by XF analysis (XFp, Seahorse Agilent, MA). The plate was subsequently centrifuged (1500×*g*/10 min) to form a monolayer in the well. After that, the supernatant was removed and replaced by XF assay medium supplemented with 1 mM sodium pyruvate, 5.5 mM D-glucose and 4 mM L-glutamine (pH 7.4). The measurements started after equilibration of the plate (10 min at 37 °C). Generally, three baseline measurements and three response rates (after the addition of a compound) were measured and the average of these rates used for data analysis. PLTs were first titrated with 0.5–2 µM of carbonyl cyanide *p*-(trifluoro-methoxy) phenyl-hydrazone (FCCP), a compound that increments oxygen consumption rate (OCR) by inhibiting the coupling between the electron transport and phosphorylation reactions [25]. One with seventy-five µM FCCP induced the greatest OCR increment that we were able to observe (Fig. S1 a, b). On the other hand, 2.5 µM of oligomycin, an inhibitor of ATP synthase, rendered the maximum inhibition of the OCR. Therefore, these concentration of FCCP and oligomycin were used for all the experiments. PLTs were consecutively treated with oligomycin A, FCCP, and antinomycin A/rotenone (0.5 µM). Experiments consisted of mixing (60 s) and measurement (3 min) cycles. All experiments were performed at 37 °C. The response to thrombin (0.5 Units/mL) was evaluated and optimal concentration of FCCP under these condition was determined by concentration response experiments as described above. In order to compare different animals/groups, and due to the fact that common methods for normalization (Hoechst staining or total protein/well) can not be used because PLTs have no nucleus and the XFp microplates are pretreated with PEI that interferes with the reagents to quantify proteins, absolute OCR values expressed as [pmolO_2/min] were normalized to the average baseline value of PLTs from WT rats obtained before the addition of thrombin, inhibitors or uncouplers and after correction of non-mitochondrial respiration (antimycin A/rotenone resistant respiration). Values were expressed as % WT Basal (100%). The respiratory parameters were calculated as previously described [26].

Hippocampal, Plasma and PLTs Expression of Human Aβ Isoforms

MSD® V-PLEX PLUS Aβ Peptide Panel 1 kit was employed to quantify soluble human Aβ 38/40/42 isoforms in plasma, hippocampal and PLTs homogenates from Tg(+/+) rats, following manufacturer's instructions. It is of note that PLTs from Tg(+/+) rats do not express the human APP transgene, and the rationale to assess human Aβ isoforms in these preparations was to determine whether rat PLTs absorb human Aβ circulating in plasma. Homogenates were performed in RIPA buffer (150 mM NaCl, 0.5% sodium deoxycholate, 1% TritonX-100, 2% SDS) containing proteases inhibitors (5 mM EDTA, 5 mM EGTA, 5 µg/mL leupeptin, 10 µg/mL aprotinin,1 µg/mL pepstatin) and phosphatases inhibitors (50 mM sodium fluoride and 5 mM sodium orthovanadate). Briefly, samples were loaded in duplicates onto MULTI-SPOT® microplates pre-coated with antibodies specific to the C-termini of Aβ38, Aβ40 and Aβ42 and were detected with SULFO-TAG™-labeled 6E10 antibody. Light emitted upon electrochemical stimulation was read using the MSD QuickPlex SQ120 instrument. Data were analyzed using MSD Workbench 4.0 software.

Evaluation of Brain Aβ Pathology and Oxidative Stress

Immunohistochemistry on freely floating (40 µm) coronal brain sections was performed as previously described [20, 27, 28] with some modifications. Briefly, Aβ deposition was detected with McSA1 mouse monoclonal antibody (1:100) and visualized with 0.05% diaminobenzidine/0.01% hydrogen peroxide (Vector Laboratories, Burlingame, USA). Oxidative damage was assessed using a monoclonal antibody against 8-hydroxy-2′-deoxyguanosine (8-OHdG) (1:50, Percipio Biosciences), a marker of nuclear and mitochondrial DNA oxidation. Immunoreactivity was developed with a secondary antibody labeled with biotin (1:250; Jackson ImmunoResearch) followed by Cy3-streptavidin (1:250; Jackson ImmunoResearch). Sections were analyzed with an Olympus BX50 microscope and/or Zeiss Pascal LSM 5 confocal microscope with LSM5 image browser.

Statistical Analyses

Group means were compared by unpaired Student t- or Mann–Whitney tests. A two-tailed probability of 5% or less was considered to be significant. Data are presented as the means ± standard error of the mean (SEM). Statistical

analyses were performed using SPSS 15.0 for Windows software (Chicago, IL, USA).

Results

Tg(+/+) Brains Display Aβ Accumulation and Markers of Oxidative Damage

It was previously reported that McGill-R-Thy1-APP homozygous transgenic rats show progressive cognitive impairments starting at the pre-plaque stage, at the age of 3 months, while amyloid plaques can be detected from 6 to 9 months of age. A revision of the cognitive domains affected in this animal model of AD-like amyloid pathology is detailed in Table 1. At a neuropathological level, brains of post-plaque Tg(+/+) rats are characterized by the presence of intraneuronal Aβ accumulation, dense amyloid plaques, astrocytosis and microglial activation and proliferation [20, 21, 29–35]. Accordingly, in our cohorts, sections of 12–14 month-old Tg(+/+) rats were positive for Aβ immunostaining (Fig. 1a, right panel) and showed increased immunoreactivity when probed with anti-8-OHdG (Fig. 1a, right panel inset), suggesting that in addition to Aβ accumulation brains of these animals display oxidation of mitochondrial nucleic acids. In agreement with neuropathology, quantitation of total Aβ levels by a highly sensitive multiplex ELISA showed that Aβ38, Aβ40 and Aβ42 human isoforms accumulate in Tg(+/+) brains (Fig. 1b, left panel).

Platelets From Tg(+/+) Rats Do Not Adsorb Human Aβ and Display Similar Coagulogram, Aggregation Profile and Mitochondrial Content as Compared to Control Animals

In accordance with the brain accumulation of human Aβ isoforms, we detected human peptides in plasma of Tg(+/+) rats (Fig. 1b, right panel) while no signal was observed in PLTs homogenates (data not shown). Regarding biochemical properties of Tg(+/+) PLTs we found a significant increment in the plateletcrit (volume occupied by platelets in the blood) of Tg(+/+) as compared to WT rats, while other aspects remained unchanged (Table 2). Moreover, the coagulogram (Table 2) and PLTs aggregation of Tg(+/+) rats was unaltered as compared to WT (Fig. 2a). In addition, the levels of ATP synthase β subunit (detected by Western blotting) were unmodified between genotypes (Fig. 2b) suggesting similar mitochondrial content in PLTs from different genotype.

Platelets From Tg(+/+) Rats Show Decreased Respiration After FCCP Addition and Impairment to Meet the Energetic Demand Associated With Thrombin-Dependent Aggregation

To determine whether mitochondrial respiration was altered in PLTs from Tg(+/+) rats we first performed a titration of FCCP using WT PLTs from 3-month-old rats in the presence of 2.5 μM oligomycin (Fig. S1a). The chosen optimal FCCP concentration (1.75 μM) was used to compare the basal respiration with that observed after FCCP addition between PLTs from 3 to 6 months WT and Tg(+/+) rats under resting conditions (Fig. 3a). We did not find significant differences in PLTs respiratory parameters between WT and Tg(+/+) rats. In both groups, respiration after FCCP addition reached basal values, but did not exhibit spare respiratory capacity, suggesting that mitochondria of resting PLTs cannot respond to an increase in energy demand. After that we evaluated the impact of aging in PLTs mitochondrial function and found that respiration after FCCP addition did not reach basal value (100%) either in WT (62.3 ± 7.68%) or Tg(+/+) (36.3 ± 8.05%) animals of 12–14 months of age (Fig. 3a). Moreover, a significant decrement was detected in Tg(+/+) as compared to WT PLTs (63.7% vs. 37.7%; $p < 0.05$).

To assess whether there were differences between genotype on PLTs plasticity in aged animals we evaluated the typical OCR and the extracellular acidification rate (ECAR) profiles after the sequential addition of thrombin (0.5 U/mL), oligomycin, FCCP and antimycin A/rotenone. The optimal FCCP concentration in thrombin-activated PLTs was determined by a new tritation (Fig. S1b) and it was the

Table 1 Cognitive deficits in homozygous transgenic McGill-R-Thy1-APP rat at the post-plaque stage

Impaired memory/learning	Behavioral task employed	References
Episodic-like memory	Novel object recognition	[35] [33] [29]
	Novel object location	[35] [33]
Spatial learning/memory	Morris water maze	[21] [29] [22]
Associative learning	Contextual fear conditioning recall	[35]
	Cued fear conditioning recall	[35]

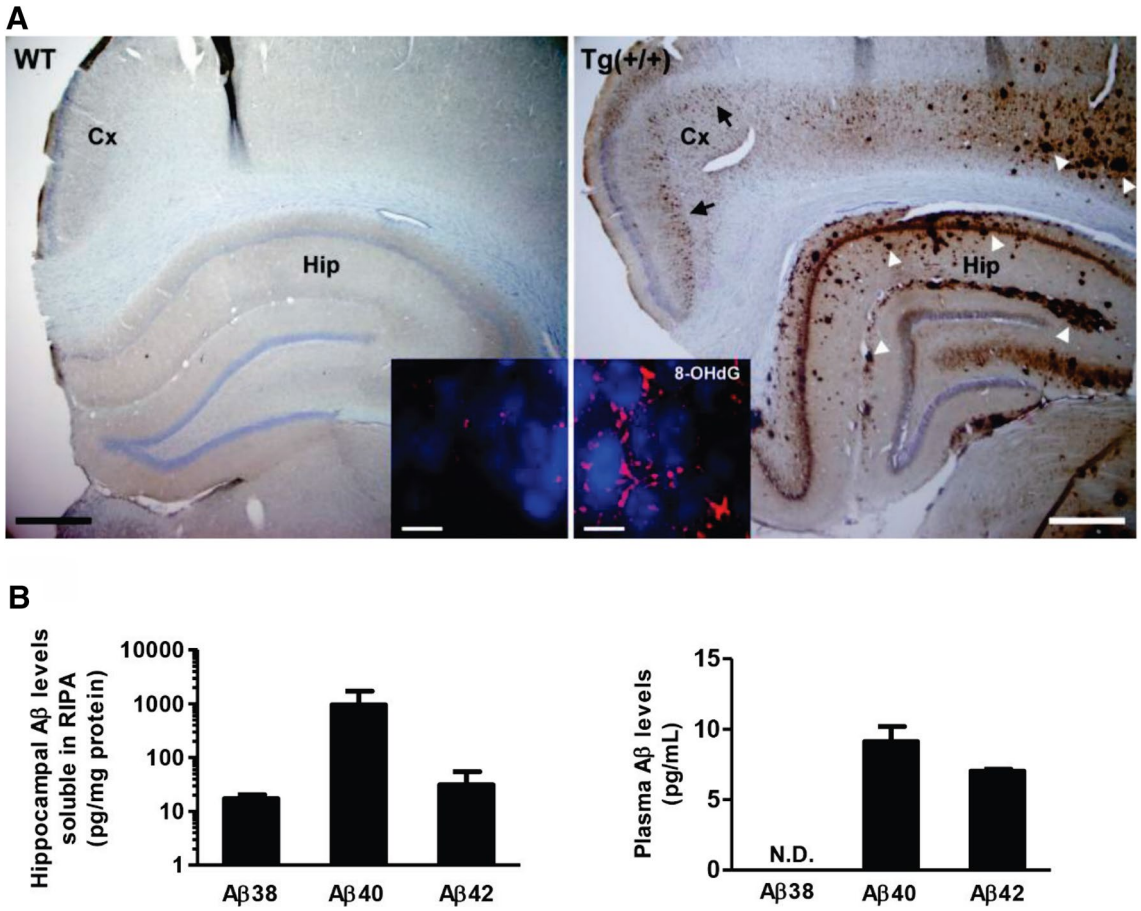

Fig. 1 Aβ pathology and oxidative stress in hippocampus of Tg(+/+) rats. **a** Intraneuronal accumulation of Aβ (arrows) and senile plaques (arrowheads) are well established neuropathological hallmarks of 12–14 month-old Tg(+/+) rats. Hippocampus (Hip) and cortex (Cx) show intense McSA1 immunoreactivity (upper right panel) as compared to age-matched WT rats (upper left panel). Sections were counterstained with cresyl violet. Insets, magnification of CA1 region decorated with 8-OHdG (red); nuclei were stained with DAPI (blue). Scale bar: 500 µm. Insets: 10 µm. **b** Aβ38/40/42 levels quantified by high sensitive multiplex ELISA in hippocampus (left panel) and plasma (right panel). Bars represent the mean ± SEM of Tg(+/+) (n = 3) rats. *ND* not detectable. (Color figure online)

Table 2 Hematologic indices in 12–14 month-old *Wistar* rats

Parameter	Units	Control (WT)	Transgenic (+/+)
Hemogram			
Platelet number	10^3/µL	508.3 ± 36.2	596.8 ± 102.4
Mean platelet volume (MPV)	Femtoliters (fL)	7.567 ± 0.1	7.400 ± 0.06
Mean platelet mass (MPM)	pg	1.403 ± 0.03	1.463 ± 0.05
Platelet volume distribution width (PDW)	Percentage (%)	37.03 ± 4.7	36.63 ± 1.4
Plateletcrit (PCT)	Percentage (%)	0.35 ± 0.01	0.54 ± 0.09*
Mean platelet component (MPC)	Gram/decilitre (g/dL)	19.5 ± 0.18	20.6 ± 0.83
Coagulogram			
PT (extrinsic pathway)	Sec	39.10 ± 5.9	38.73 ± 8.2
PT	%	23.17 ± 5.2	24.17 ± 4.8
INR		3.6 ± 0.6	3.5 ± 0.8
aPTT (intrinsic pathway)	Sec	37.3 ± 16.3	29.6 ± 8.1

MPV analyser-calculated measure of thrombocyte volume, *MPM* mean platelet mass, *PDW* Indicator of volume variability in platelets size, *PCT* Volume occupied by platelets in the blood, *MPC* Measure of mean refractive index of the platelets. *PT* prothrombin time test, *aPTT* activated partial thromboplastin time, *INR* international normalized ratio. n = 3–6 rats/ group

*$p < 0.05$

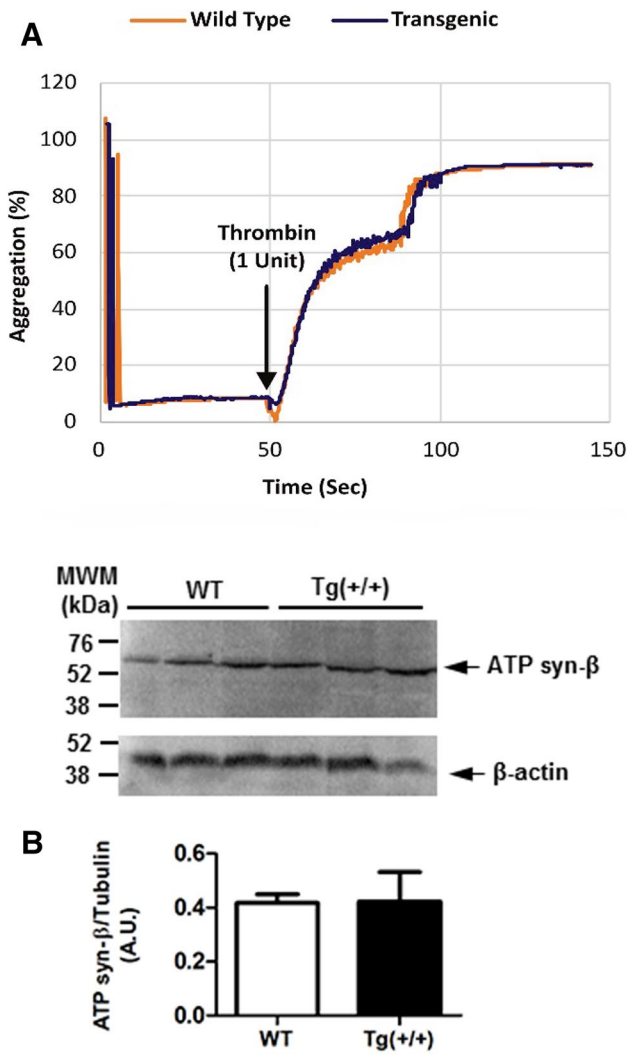

Fig. 2 Platelets from aged Tg(+/+) rats show similar aggregation profile and mitochondrial content as compared to WT animals. **a** The graph shows a representative aggregation profile of washed rat PLTs under resting conditions and in the presence of agonist (1 Unit of human thrombin) while stirring. Orange line, WT; blue line, Tg(+/+). **b** Representative Western blot of PLTs corresponding to WT and Tg(+/+) rats probed with mitochondrial resident protein ATP synthase β subunit and β-actin, respectively. Left, molecular mass markers in kDa. Lower panel, bars represent the mean ± SEM of the immunoreactivity of ATP synthase β subunit normalized by β-actin expressed as arbitrary units (AU). (Color figure online)

same as under resting conditions (1.75 μM). In this context, the injection of thrombin increased the basal OCR in PLTs from WT and Tg(+/+) rats (Fig. 3b). By contrast to thrombin-activated PLTs from WT rats, thrombin-activated PLTs from Tg(+/+) did not reach basal OCR after FCCP addition (Fig. 3b). Again, no spare respiratory capacity was detected in thrombin activated PLTs from either WT or Tg(+/+) rats. To measure non-mitochondrial sources of oxygen consumption, the mitochondrial complex III and I inhibitors, antimycin A (0.5 μM) and rotenone (0.5 μM), respectively, were injected 12 min after FCCP addition, and caused, as expected, a decrease in the OCR in both groups (Fig. 3b).

The basal ECAR (100%) increased similarly in WT and Tg(+/+) rats in response to thrombin and it was found to be augmented approximately by 379% and 318%, respectively. Moreover, increments of 454% (WT) and 363% (Tg(+/+)) were observed after oligomycin addition in agreement with the activation of anaerobic glycolysis in response to the inhibition of mitochondrial ATP synthesis (Fig. 3c).

To determine whether mitochondrial metabolic parameters were statistically different between genotypes in aged rats, absolute values were normalized to the average baseline value of PLTs from WT rats obtained before the addition of thrombin, inhibitors or uncouplers and after correction of non-mitochondrial respiration. As it is shown in Fig. 3d the injection of thrombin significantly increased basal OCR in WT PLTs (172%) while the increment in Tg(+/+) PLTs (127%) was similar to WT basal respiration (100%). We also found in thrombin activated WT PLTs a significant increment in the respiration reached after FCCP addition, as compared to resting conditions (130% vs. 100%). By contrast, a significant decrement was detected in thrombin activated PLTs from Tg(+/+) (49%) as compared to WT rats (100%) (Fig. 3d). The fact that proton leak was unchanged between PLTs from WT and Tg(+/+) rats under either resting or activated conditions (Fig. 3a and d), suggests that mitochondria were not damaged in PLTs from Tg(+/+) rats.

Discussion

To the extent of our knowledge, this is the first report to study PTLs mitochondrial function in a transgenic model of AD. At the hematological level, the only parameter that differed significantly in the hemogram between WT and Tg(+/+) rats was the plateletcrit (PCT), suggesting that the volume occupied by PLTs in the blood of Tg(+/+) is higher than in WT rats. However, as the mean PLTs number and PLT volume did not differ significantly between genotypes we could suggest that mean PCT values of WT (0.35%) and Tg(+/+) (0.54%) are included in the interval of reference values of Wistar rats similar to what was reported in Sprague–Dawley rats [36].

At the functional level we show that PLTs from Tg(+/+) rats did not display any alterations in the rate of aggregation at baseline or after the addition of thrombin as agonist. In this regard, it was previously reported that inhibition of mitochondrial metabolism do not prevent PLTs aggregation, probably due to a switch to glycolytic metabolism, to compensate for the decrease in oxidative phosphorylation. Furthermore combining inhibition of glycolysis, with inhibition of fatty acid metabolism and/or glutamine depletion, strongly inhibits aggregation, compared to glycolytic

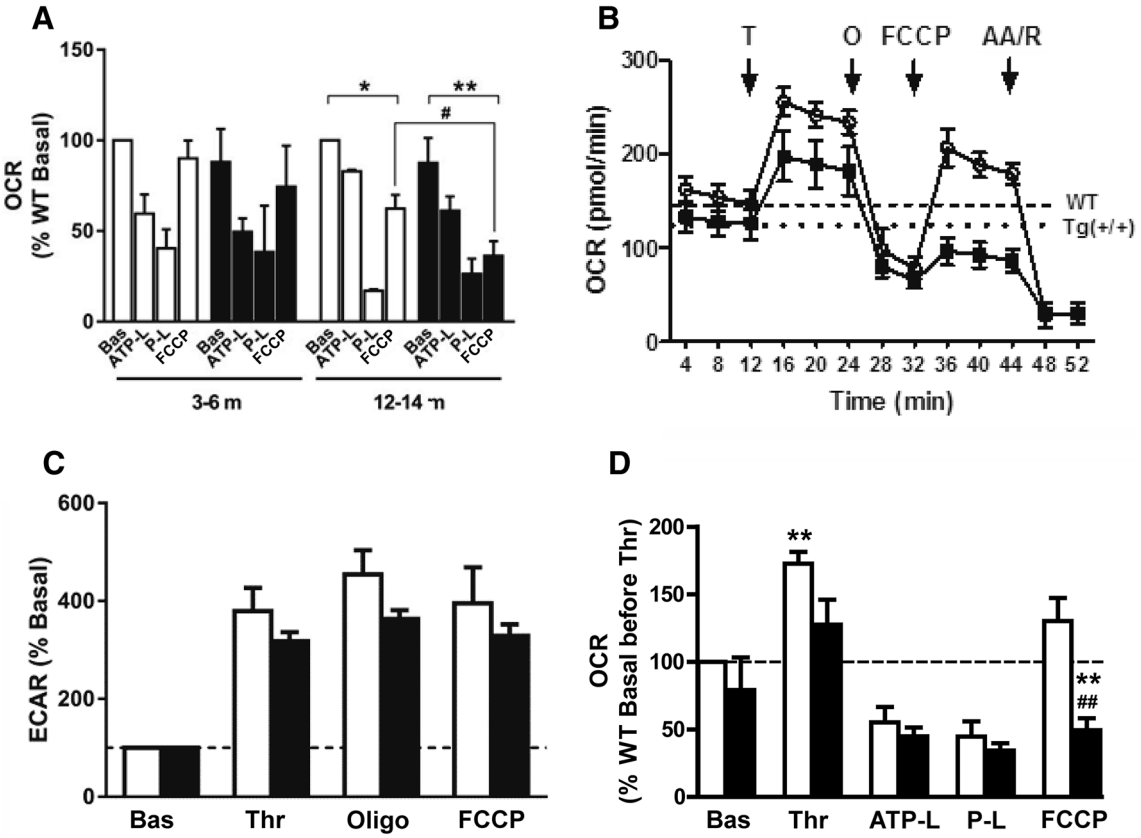

Fig. 3 Bioenergetic profile of PLTs from WT and Tg(+/+) rats. **a** Parameters of mitochondrial function were calculated in resting PLTs. OCR was normalized to the average baseline value of PLTs from WT rats obtained before the addition of inhibitors or uncouplers and after correction of non-mitochondrial respiration. Values are expressed as % WT Basal (100%). White bars, WT; black bars, Tg(+/+). Data are expressed as the mean ± SEM of WT (n = 4) and Tg(+/+) (n = 5) rats. Three replicates per sample were performed. $^{*}p < 0.05$, respiration after FCCP addition versus basal respiration (100%) in 12–14 month-old WT rats; $^{**}p < 0.01$, respiration after FCCP addition vs. basal respiration in 12–14 month-old Tg (+/+) rats; $^{\#}p < 0.05$, respiration after FCCP addition between 12 and 14 month-old WT and Tg (+/+) rats. **b** OCR profile of thrombin-activated PLTs. Circle, WT; square, Tg(+/+). PLTs basal respiration was determined during 12 min. After that, thrombin (T) was applied and then sequential injections of oligomycin (O), FCCP and Antimycin A (AA)/Rotenone (R) were performed. Dashed and dotted lines represent the basal respiration for PLTs from WT and Tg(+/+) rats, respectively. **c** Graph bars shows the extracellular acidification rate (ECAR) determined in parallel with respiration shown in **b**. Data are expressed as the mean % of basal (100%) ± SEM. WT, white bars (n = 4); Tg(+/+), black bars (n = 5) rats. Three replicates per sample were performed. **d** Parameters of mitochondrial function were calculated in thrombin-activated PLTs from 12 to 14 WT and Tg(+/+) rats. OCR was normalized to the average baseline value of PLTs from WT rats obtained before the addition of thrombin, inhibitors or uncouplers and after correction of non-mitochondrial respiration. Values are expressed as % WT Basal (100%). White bars, 12–14 month-old WT rats; Black bars, 12–14 month-old Tg(+/+) rats. Data are expressed as the mean ± SEM of WT (n = 4) and Tg(+/+) (n = 5) rats. Three replicates per sample were performed. $^{**}p < 0.01$ WT basal respiration (100%) versus WT basal respiration after thrombin addition; $^{**}p < 0.01$ respiration after FCCP addition between WT and Tg(+/+) rats; $^{\#\#}p < 0.01$ respiration after FCCP addition in Tg(+/+) rats versus WT basal respiration (100%). *Bas*. (Basal OCR— non-mitochondrial OCR); *Thr* (OCR after thrombin addition—non-mitochondrial OCR); *ATP-L*, ATP-linked respiration (Basal—Oligomycin resistant OCR); *P-L*, proton-Leak (Oligomycin resistant OCR—non-mitochondrial OCR); *FCCP*, respiration after FCCP addition (OCR after the addition of FCCP—non-mitochondrial OCR)

inhibition alone, providing further evidence for multiple oxidative substrate usage in platelet metabolism [37].

Our results show that the presence of the transgen did not alter the mitochondrial content in PLTs homogenates suggesting that differences in the metabolism of PLTs from Tg(+/+) rats as compared to WT could be assigned to mitochondria dysfunction as previously suggested in PLTs isolated from AD patients [38].

Here we report that under resting conditions, there are no significant differences in any of the bioenergetics parameters, analyzed between WT and Tg(+/+) PLTs isolated from young animals (3–6 months of age). It is of note that PLTs from WT and Tg(+/+) rats do not exhibit spare respiratory capacity in agreements with previous reports [39, 40], suggesting that mitochondria of resting PLTs cannot respond to an increase in energy demand. In addition,

in 12–14 month-old rats respiration after FCCP addition did not reach basal values regardless the genotype analyzed, suggesting that aging may modulate PLTs bioenergetics. Moreover, respiration after FCCP addition showed a significant decrease in PLTs from 12 to 14 month-old Tg(+/+) as compared to WT rats, suggesting that Aβ and or APP fragments accumulation in the brain may generate an oxidative/inflammatory environment that promotes PLTs mitochondrial dysfunction that mirrors bioenergetics defect observed in the brain of Tg(+/+) rats. We have previously demonstrated that the hippocampus of 6 month-old hemizygous transgenic rats shows alterations of redox equilibrium and sustained mitochondrial oxidative damage which may be responsible of the respiratory impairments observed in synaptosomes [28]. In the present work, we provide strong evidence that the hippocampus of aged Tg(+/+) rats shows Aβ plaques and expression of 8-OHdG positive cells in brain areas displaying Aβ accumulation in a pattern similar to what was observed in AD brains [41] and that both brain biomarkers impact on the bioenergetics performance of PLTs.

The fact that resting PLTs do not display spare respiratory capacity is in agreement with the physiological role of this blood component. By contrast to neurons, that generally maintain a reserve capacity that enables upregulation of energy production under conditions of stress or excess energy demand [42] and in which the lack of reserve capacity have been linked to increased sensitivity to cell death in the presence of stressors [43, 44], resting PLTs do not face any energy request.

Interestingly, thrombin significantly increased basal respiration in PLTs from aged WT rats, indicating the contribution of the mitochondrion to the energetic request associated with thrombin stimulated aggregation. However, this phenotype was not observed in PLTs of aged Tg(+/+) animals. Taking into account that we did not find differences in the aggregation profile between PLTs from WT and Tg(+/+) rats we could speculate that PLTs from Tg(+/+) rats could compensate the energetic demand with glycolysis as previously reported [37]. Further experiments are required to test this hypothesis.

The significant decrements detected in respiration after FCCP addition between thrombin-activated PLTs from Tg(+/+) and WT rats may reflects the failure of Tg(+/+) PLTs to respond to an increase in energy demand with the same performance than WT PLTs, suggesting reduced fitness or flexibility. It is of note that decreased respiration observed after FCCP addition in thrombin-activated PLTs from Tg(+/+) rats was previously reported in synaptosomes isolated from transgenic rat brains when challenged with an increased energy demand [28], suggesting that the poor performance of these animals in hippocampal-dependent tasks [27] may be due to this synaptic metabolic impairment.

Decrements observed in respiration after FCCP addition is consistent with a potential deficit of substrates, taking into account that the XF base medium used in these experiments contains only pyruvate, glutamine and glucose, but not free fatty acids. Substrates involved in the rapid and sustained stimulation of mitochondrial respiration upon addition of thrombin in PLTs are unknown. One possibility is that they are fatty acids likely derived from endogenous free fatty acids and from triglycerides stores [45, 46]. Fatty acid oxidation also occurs in peroxisomes and in the presence of enzymes such as cyclooxygenase [47, 48]. However, since the OCR is inhibited by antimycin A/rotenone, we consider that it can largely be ascribed to mitochondrial oxidative phosphorylation. It has been suggested that high levels of thrombin lead to the opening of the mitochondrial permeability transition pore during PLTs aggregation, inducing a decrement in the mitochondrial membrane potential and a reduction of the ATP output [49, 50]. In this report, we have shown that over the first 20 min after thrombin exposure there is no change in proton leak, suggesting that in PLTs from WT and Tg(+/+) rats the mitochondrial permeability transition pore was not opened under these conditions.

A previous metabolic study using PLTs from AD patients suggested that changes in mitochondrial respiratory parameters are not associated with the progression of AD, except for the increased capacity of the electron transport system in digitonin permeabilized PLTs [38]. By contrast, our data show a significant decrease in the respiration after FCCP addition in intact PLTs from Tg(+/+) as compared to WT rats. Discrepancy between our data and those reported previously in AD patients may be due to differences in the methodologies employed and/or in intrinsic properties of biological samples. Fišar et al. [38] performed experiments in an Oroboros Oxygraph with continuous stirring in a buffer with mitochondrial substrates (malate, pyruvate, ADP, glutamate and succinate), while the measurement with the Seahorse extracellular flux analyzer employed in the present study was carried out with PLTs seeded in miniplates and relied on the presence of glucose that needs to be processed by PLTs prior to be used as mitochondrial substrate, resembling a more physiological situation. Moreover, human PLTs are able to generate endogenous Aβ [14] with potential amyloidogenic and toxic properties, while PLTs of Tg(+/+) generates rodent Aβ which is non-amyloidogenic [51] and not toxic.

In conclusion, in the present study we show that thrombin activated PLTs from aged Tg(+/+) rats exhibit a specific profile of mitochondrial dysfunction, even if PLTs of Tg(+/+) rats do not accumulate Aβ. Tg(+/+) brain displays oxidative and nitrosative stress markers, protein-bound 4-hydroxynonenal and protein-resident 3-nitrotyrosine which generate inflammatory cytokine production (TNF-α and IFN-ϒ), as well as microglial recruitment towards Aβ-burdened neurons [52]. Cytokines produced in the CNS can enter the

circulation with the reabsorption of the CSF. Moreover, the nonsaturable efflux from the CSF to blood may result in large increases in blood levels of cytokines [53]. We propose that PLTs from Tg(+/+) rats, containing respiring mitochondria, sense and respond to cytokines such as TNF-α which induces PLTs reactive oxygen species (O_2^-) production [54] that may damage the respiratory chain complexes leading to bioenergetics dysfunction. Since mitochondria of PLTs cannot be replaced, they have frequently been used as a bioenergetics sensor of pathological setting. The failure to remove damaged mitochondria by mitophagy and replace them with healthy organelles can result in a progressive deterioration in PLTs bioenergetics function [18] as here reported in a model of a chronic disease.

Furthermore, the association of PLTs metabolic alterations with neuropathology and cognitive impairments observed in this animal model suggests that PLTs bioenergetics may potentially be useful to assess clinical severity and progression in AD patients.

Acknowledgements We acknowledge the helpful assistance of the personnel of the Laboratory of Hospital Naval Cirujano Dr. Pedro Mallo (Ciudad de Buenos Aires-Argentina) on the determination of the haematologic indices in animals. We wish to thank Dr. Mirta Schattner and Dr. Roberto G. Pozner of the Laboratory of Experimental Thrombosis-Academia Nacional de Medicina (Ciudad de Buenos Aires-Argentina) for their support on the evaluation of platelet aggregation.

Funding This study was supported by funding from the Agencia Nacional de Promoción Científica y Tecnológica (Grant Nos. PICT-2015-0285, PICT-2016-4647 and PIBT/09 2013 to LM; PICT-2013-318 to EMC), Consejo Nacional de Investigaciones Científicas y Técnicas (Grant No. PIP-0378 to LM), Canadian Institutes of Health Research (Grant Nos. 201603PJT-364544 to ACC). FAP is supported by FONCyT fellowship. PVMA is supported by CONICET fellowship. PG, EMC, and LM are members of the Research Career of CONICET. SDC is the holder of the Charles E. Frosst/Merck Research Associate position. ACC is member of the Canadian Consortium of Neurodegeneration in Aging (CCNA) and holder of the McGill University Charles E. Frosst/Merck Chair in Pharmacology.

References

1. Alzheimer's Association (2013) Alzheimer's disease facts and figures. Alzheimers Dement 9:208–245. https://doi.org/10.1016/j.jalz.2013.02.003
2. Hardy J, Selkoe DJ (2002) The amyloid hypothesis of Alzheimer's disease: progress and problems on the road to therapeutics. Science 297:353–356. https://doi.org/10.1126/science.1072994
3. Aisen PS, Andrieu S, Sampaio C, Carrillo M, Khachaturian ZS, Dubois B, Feldman HH, Petersen RC, Siemers E, Doody RS, Hendrix SB, Grundman M, Schneider LS, Schindler RJ, Salmon E, Potter WZ, Thomas RG, Salmon D, Donohue M, Bednar MM, Touchon J, Vellas B (2011) Report of the task force on designing clinical trials in early (predementia) AD. Neurology 76:280–286. https://doi.org/10.1212/WNL.0b013e318207b1b9
4. Zhang XL, Liu XJ, Hu SS, Thomas S, Tian YQ, Gao RL, Wu QY, Wei HX, Yang XB, Wang H, He ZX, Schelbert HR (2008) Impact of viable myocardium assessed by 99Tcm-MIBI SPECT and 18F-FDG PET imaging on clinical outcome of patients with left ventricular aneurysm underwent revascularization. Zhonghua Xin Xue Guan Bing Za Zhi 36:999–1003. https://doi.org/10.3321/j.issn:0253-3758.2008.11.010
5. Baird AL, Westwood S, Lovestone S (2015) Blood-based proteomic biomarkers of Alzheimer's disease pathology. Front Neurol 6:236. https://doi.org/10.3389/fneur.2015.00236
6. Pletscher A, Laubscher A (1980) Blood platelets as models for neurons: uses and limitations. J Neural Transm Suppl 16:7–16. https://doi.org/10.1007/978-3-7091-8582-7_2
7. Talib LL, Joaquim HP, Forlenza OV (2012) Platelet biomarkers in Alzheimer's disease. World J Psychiatry 2:95–101. https://doi.org/10.5498/wjp.v2.i6.95
8. Behari M, Shrivastava M (2013) Role of platelets in neurodegenerative diseases: a universal pathophysiology. Int J Neurosci 123:287–299. https://doi.org/10.3109/00207454.2012.751534
9. Machlus KR, Thon JN, Italiano JE (2014) Interpreting the developmental dance of the megakaryocyte: a review of the cellular and molecular processes mediating platelet formation. Br J Haematol 165:227–236. https://doi.org/10.1111/bjh.12758
10. Yun SH, Sim EH, Goh RY, Park JI, Han JY (2016) Platelet activation: the mechanisms and potential biomarkers. Biomed Res Int 2016:9060143. https://doi.org/10.1155/2016/9060143
11. Jennings LK (2009) Mechanisms of platelet activation: need for new strategies to protect against platelet-mediated atherothrombosis. Thromb Haemost 102:248–257. https://doi.org/10.1160/TH09-03-0192
12. Ponomarev ED (2018) Fresh evidence for platelets as neuronal and innate immune cells: their role in the activation, differentiation, and deactivation of Th1, Th17, and Tregs during tissue inflammation. Front Immunol 9:406. https://doi.org/10.3389/fimmu.2018.00406
13. Casoli T, Di Stefano G, Giorgetti B, Grossi Y, Balietti M, Fattoretti P, Bertoni-Freddari C (2007) Release of beta-amyloid from high-density platelets: implications for Alzheimer's disease pathology. Ann N Y Acad Sci 1096:170–178. https://doi.org/10.1196/annals.1397.082
14. Catricala S, Torti M, Ricevuti G (2012) Alzheimer disease and platelets: how's that relevant. Immun Ageing 9:20. https://doi.org/10.1186/1742-4933-9-20
15. Davies TA, Long HJ, Eisenhauer PB, Hastey R, Cribbs DH, Fine RE, Simons ER (2000) Beta amyloid fragments derived from activated platelets deposit in cerebrovascular endothelium: usage of a novel blood brain barrier endothelial cell model system. Amyloid 7:153–165. https://doi.org/10.3109/13506120009146830
16. Di Luca M, Colciaghi F, Pastorino L, Borroni B, Padovani A, Cattabeni F (2000) Platelets as a peripheral district where to study pathogenetic mechanisms of alzheimer disease: the case of amyloid precursor protein. Eur J Pharmacol 405:277–283. https://doi.org/10.1016/S0014-2999(00)00559-8
17. Tyrrell DJ, Bharadwaj MS, Jorgensen MJ, Register TC, Shively C, Andrews RN, Neth B, Keene CD, Mintz A, Craft S, Molina AJA (2017) Blood-based bioenergetic profiling reflects differences in brain bioenergetics and metabolism. Oxid Med Cell Longev 2017:7317251. https://doi.org/10.1155/2017/7317251
18. Chacko BK, Kramer PA, Ravi S, Benavides GA, Mitchell T, Dranka BP, Ferrick D, Singal AK, Ballinger SW, Bailey SM, Hardy RW, Zhang J, Zhi D, Darley-Usmar VM (2014) The Bioenergetic Health Index: a new concept in mitochondrial translational research. Clin Sci (Lond) 127:367–373. https://doi.org/10.1042/CS20140101
19. Gotz J, Ittner LM (2008) Animal models of Alzheimer's disease and frontotemporal dementia. Nat Rev Neurosci 9:532–544. https://doi.org/10.1038/nrn2420
20. Leon WC, Canneva F, Partridge V, Allard S, Ferretti MT, DeWilde A, Vercauteren F, Atifeh R, Ducatenzeiler A, Klein

W, Szyf M, Alhonen L, Cuello AC (2010) A novel transgenic rat model with a full Alzheimer's-like amyloid pathology displays pre-plaque intracellular amyloid-beta-associated cognitive impairment. J Alzheimers Dis 20:113–126. https://doi.org/10.3233/JAD-2010-1349
21. Parent MJ, Zimmer ER, Shin M, Kang MS, Fonov VS, Mathieu A, Aliaga A, Kostikov A, Do Carmo S, Dea D, Poirier J, Soucy JP, Gauthier S, Cuello AC, Rosa-Neto P (2017) Multimodal imaging in rat model recapitulates Alzheimer's disease biomarkers abnormalities. J Neurosci 37:12263–12271. https://doi.org/10.1523/JNEUROSCI.1346-17.2017
22. Mustard JF, Kinlough-Rathbone RL, Packham MA (1989) Isolation of human platelets from plasma by centrifugation and washing. Methods Enzymol 169:3–11
23. Garcia-Manzano A, Gonzalez-Llaven J, Lemini C, Rubio-Poo C (2001) Standardization of rat blood clotting tests with reagents used for humans. Proc West Pharmacol Soc 44:153–155
24. Rivadeneyra L, Carestia A, Etulain J, Pozner RG, Fondevila C, Negrotto S, Schattner M (2014) Regulation of platelet responses triggered by Toll-like receptor 2 and 4 ligands is another non-genomic role of nuclear factor-kappaB. Thromb Res 133:235–243. https://doi.org/10.1016/j.thromres.2013.11.028
25. Terada H (1990) Uncouplers of oxidative phosphorylation. Environ Health Perspect 87:213–218. https://doi.org/10.1289/ehp.9087213
26. Brand MD, Nicholls DG (2011) Assessing mitochondrial dysfunction in cells. Biochem J 435:297–312. https://doi.org/10.1042/BJ20110162
27. Galeano P, Martino Adami PV, Do Carmo S, Blanco E, Rotondaro C, Capani F, Castano EM, Cuello AC, Morelli L (2014) Longitudinal analysis of the behavioral phenotype in a novel transgenic rat model of early stages of Alzheimer's disease. Front Behav Neurosci 8:321. https://doi.org/10.3389/fnbeh.2014.00321
28. Martino Adami PV, Quijano C, Magnani N, Galeano P, Evelson P, Cassina A, Do Carmo S, Leal MC, Castano EM, Cuello AC, Morelli L (2017) Synaptosomal bioenergetic defects are associated with cognitive impairment in a transgenic rat model of early Alzheimer's disease. J Cereb Blood Flow Metab 37:69–84. https://doi.org/10.1177/0271678X15615132
29. Hall H, Iulita MF, Gubert P, Flores Aguilar L, Ducatenzeiler A, Fisher A, Cuello AC (2018) AF710B, an M1/sigma-1 receptor agonist with long-lasting disease-modifying properties in a transgenic rat model of Alzheimer's disease. Alzheimers Dement 14:811–823. https://doi.org/10.1016/j.jalz.2017.11.009
30. Iulita MF, Bistue Millon MB, Pentz R, Aguilar LF, Do Carmo S, Allard S, Michalski B, Wilson EN, Ducatenzeiler A, Bruno MA, Fahnestock M, Cuello AC (2017) Differential deregulation of NGF and BDNF neurotrophins in a transgenic rat model of Alzheimer's disease. Neurobiol Dis 108:307–323. https://doi.org/10.1016/j.nbd.2017.08.019
31. Wilson EN, Abela AR, Do Carmo S, Allard S, Marks AR, Welikovitch LA, Ducatenzeiler A, Chudasama Y, Cuello AC (2017) Intraneuronal amyloid beta accumulation disrupts hippocampal CRTC1-dependent gene expression and cognitive function in a rat model of Alzheimer disease. Cereb Cortex 27:1501–1511. https://doi.org/10.1093/cercor/bhv332
32. Heggland I, Storkaas IS, Soligard HT, Kobro-Flatmoen A, Witter MP (2015) Stereological estimation of neuron number and plaque load in the hippocampal region of a transgenic rat model of Alzheimer's disease. Eur J Neurosci 41:1245–1262. https://doi.org/10.1111/ejn.12876
33. Pimentel LS, Allard S, Do Carmo S, Weinreb O, Danik M, Hanzel CE, Youdim MB, Cuello AC (2015) The multi-target drug M30 shows pro-cognitive and anti-inflammatory effects in a rat model of Alzheimer's disease. J Alzheimers Dis 47:373–383. https://doi.org/10.3233/JAD-143126
34. Hanzel CE, Pichet-Binette A, Pimentel LS, Iulita MF, Allard S, Ducatenzeiler A, Do Carmo S, Cuello AC (2014) Neuronal driven pre-plaque inflammation in a transgenic rat model of Alzheimer's disease. Neurobiol Aging 35:2249–2262. https://doi.org/10.1016/j.neurobiolaging.2014.03.026
35. Iulita MF, Allard S, Richter L, Munter LM, Ducatenzeiler A, Weise C, Do Carmo S, Klein WL, Multhaup G, Cuello AC (2014) Intracellular Abeta pathology and early cognitive impairments in a transgenic rat overexpressing human amyloid precursor protein: a multidimensional study. Acta Neuropathol Commun 2:61. https://doi.org/10.1186/2051-5960-2-61
36. He Q, Su G, Liu K, Zhang F, Jiang Y, Gao J, Liu L, Jiang Z, Jin M, Xie H (2017) Sex-specific reference intervals of hematologic and biochemical analytes in Sprague-Dawley rats using the nonparametric rank percentile method. PLoS ONE 12:e0189837. https://doi.org/10.1371/journal.pone.0189837
37. Ravi S, Chacko B, Sawada H, Kramer PA, Johnson MS, Benavides GA, O'Donnell V, Marques MB, Darley-Usmar VM (2015) Metabolic plasticity in resting and thrombin activated platelets. PLoS ONE 10:e0123597. https://doi.org/10.1371/journal.pone.0123597
38. Fisar Z, Hroudova J, Hansikova H, Spacilova J, Lelkova P, Wenchich L, Jirak R, Zverova M, Zeman J, Martasek P, Raboch J (2016) Mitochondrial respiration in the platelets of patients with Alzheimer's disease. Curr Alzheimer Res 13:930–941. https://doi.org/10.2174/1567205013666160314150856
39. Xu W, Cardenes N, Corey C, Erzurum SC, Shiva S (2015) Platelets from asthmatic individuals show less reliance on glycolysis. PLoS ONE 10:e0132007. https://doi.org/10.1371/journal.pone.0132007
40. Schoenwaelder SM, Darbousset R, Cranmer SL, Ramshaw HS, Orive SL, Sturgeon S, Yuan Y, Yao Y, Krycer JR, Woodcock J, Maclean J, Pitson S, Zheng Z, Henstridge DC, van der Wal D, Gardiner EE, Berndt MC, Andrews RK, James DE, Lopez AF, Jackson SP (2016) 14-3-3zeta regulates the mitochondrial respiratory reserve linked to platelet phosphatidylserine exposure and procoagulant function. Nat Commun 7:12862. https://doi.org/10.1038/ncomms12862
41. Gabbita SP, Lovell MA, Markesbery WR (1998) Increased nuclear DNA oxidation in the brain in Alzheimer's disease. J Neurochem 71:2034–2040. https://doi.org/10.1046/j.1471-4159.1998.71052034.x
42. Pfleger J, He M, Abdellatif M (2015) Mitochondrial complex II is a source of the reserve respiratory capacity that is regulated by metabolic sensors and promotes cell survival. Cell Death Dis 6:e1835. https://doi.org/10.1038/cddis.2015.202
43. Sriskanthadevan S, Jeyaraju DV, Chung TE, Prabha S, Xu W, Skrtic M, Jhas B, Hurren R, Gronda M, Wang X, Jitkova Y, Sukhai MA, Lin FH, Maclean N, Laister R, Goard CA, Mullen PJ, Xie S, Penn LZ, Rogers IM, Dick JE, Minden MD, Schimmer AD (2015) AML cells have low spare reserve capacity in their respiratory chain that renders them susceptible to oxidative metabolic stress. Blood 125:2120–2130. https://doi.org/10.1182/blood-2014-08-594408
44. Hill BG, Dranka BP, Zou L, Chatham JC, Darley-Usmar VM (2009) Importance of the bioenergetic reserve capacity in response to cardiomyocyte stress induced by 4-hydroxynonenal. Biochem J 424:99–107. https://doi.org/10.1042/BJ20090934
45. Niu X, Whisson ME, Guppy M (1997) Types and sources of fuels for platelets in a medium containing minimal added fuels and a low carryover plasma. Br J Haematol 97:908–916. https://doi.org/10.1046/j.1365-2141.1997.1442963.x
46. Derksen A, Cohen P (1975) Patterns of fatty acid release from endogenous substrates by human platelet homogenates and membranes. J Biol Chem 250:9342–9347
47. Wanders RJ, Vreken P, Ferdinandusse S, Jansen GA, Waterham HR, van Roermund CW, Van Grunsven EG (2001) Peroxisomal

fatty acid alpha- and beta-oxidation in humans: enzymology, peroxisomal metabolite transporters and peroxisomal diseases. Biochem Soc Trans 29:250–267. https://doi.org/10.1042/bst0290250
48. Marnett LJ, Rowlinson SW, Goodwin DC, Kalgutkar AS, Lanzo CA (1999) Arachidonic acid oxygenation by COX-1 and COX-2. Mechanisms of catalysis and inhibition. J Biol Chem 274:22903–22906. https://doi.org/10.1074/jbc.274.33.22903
49. Halestrap AP (2006) Calcium, mitochondria and reperfusion injury: a pore way to die. Biochem Soc Trans 34:232–237. https://doi.org/10.1042/BST20060232
50. Halestrap AP, Clarke SJ, Javadov SA (2004) Mitochondrial permeability transition pore opening during myocardial reperfusion–a target for cardioprotection. Cardiovasc Res 61:372–385. https://doi.org/10.1016/S0008-6363(03)00533-9
51. Fraser PE, Nguyen JT, Inouye H, Surewicz WK, Selkoe DJ, Podlisny MB, Kirschner DA (1992) Fibril formation by primate, rodent, and Dutch-hemorrhagic analogues of Alzheimer amyloid beta-protein. Biochemistry 31:10716–10723
52. Wilson EN, Carmo SD, Iulita MF, Hall H, Austin GL, Jia DT, Malcolm JC, Foret MK, Marks A, Butterfield DA, Cuello AC (2018) Microdose lithium NP03 diminishes pre-Plaque oxidative damage and neuroinflammation in a rat model of Alzheimer's-like amyloidosis. Curr Alzheimer Res. https://doi.org/10.2174/1567205015666180904154446
53. Banks WA (2008) Blood–brain barrier transport of cytokines. In: Phelps C, Korneva E (eds) NeuroImmune biology. Elsevier Science, Amsterdam, pp 93–106
54. De Biase L, Pignatelli P, Lenti L, Tocci G, Piccioni F, Riondino S, Pulcinelli FM, Rubattu S, Volpe M, Violi F (2003) Enhanced TNF alpha and oxidative stress in patients with heart failure: effect of TNF alpha on platelet O_2-production. Thromb Haemost 90:317–325. https://doi.org/10.1160/TH03-02-0105